CARBONATE LITHOFACIES PREDICTION USING NEURAL NETWORK AND GEOSTATISTICAL 3D MODELING OF OOLITE SHOALS, ST. LOUIS LIMESTONE, SOUTHWEST KANSAS

QI LIANSHUANG[1,2,3], TIMOTHY R. CARR[1], AND ROBERT H. GOLDSTEIN[3]

NEURAL NETWORK & LITHOFACIES PREDICTION

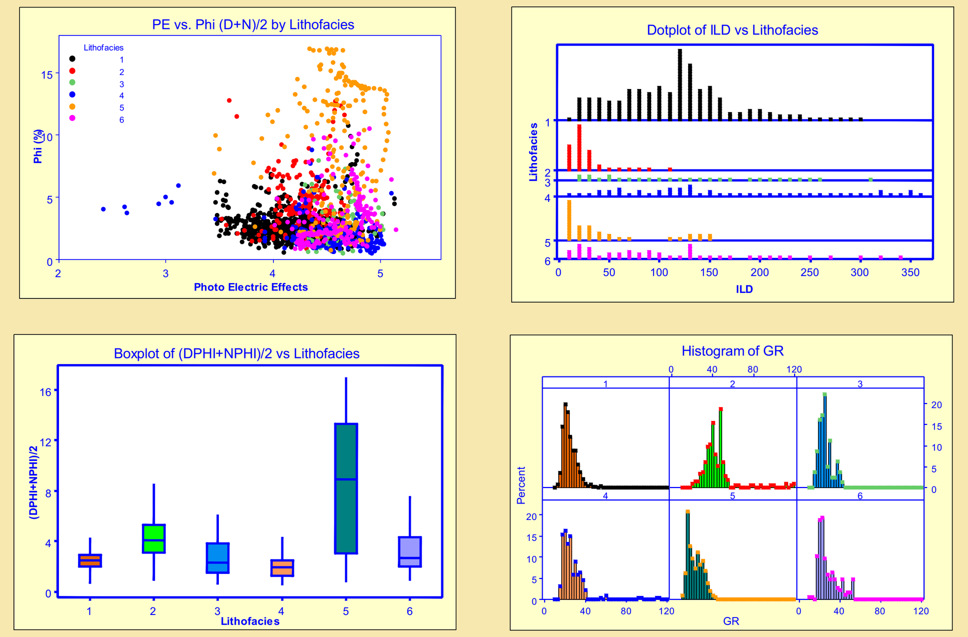

Determined predictor variables (GR, ILD, ILM, PE, NPhi, DPhi) and lithofacies categories were used to build Neural Network models. The size of network and damping parameters were optimized using cross-validation and repeat testing with whole training data and randomly chosen partial data sets.

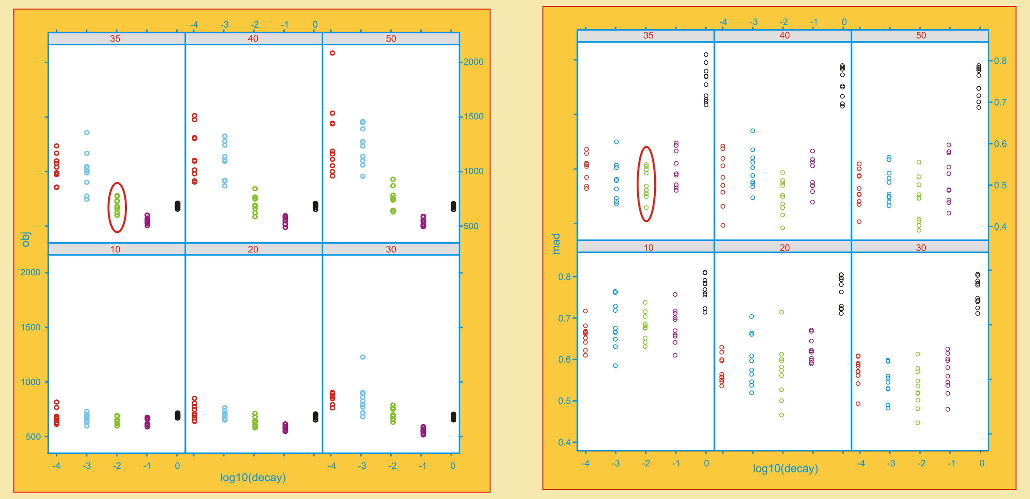

Cross validation performed on different network size and damping parameters with objective function and mad parameter, which is mean absolute difference between the predicted and actual facies number. Neural network model (size=35, damping =0.05) was selected for facies prediction.

Predicted Lithofacies Scorecard (Counts) for 10 key trained wells with PE Curve

Actural Facies		Predicted Facies 1	2	3	4	5	6	Grand Total	Absolute Accuracy	Counts within 1	Accuracy Within 1 facies
	1	1074	14	4	11	4	6	1113	96.50%	1089	97.84%
	2	15	199				1	215	92.56%	214	99.53%
	3	11	4	57	1	5	3	81	70.37%	62	76.54%
	4	26	1	1	172	5	16	221	77.83%	178	80.54%
	5	9	2	2	1	188	5	207	90.82%	194	93.72%
	6	17		1	9	7	152	186	81.72%	168	90.32%
	Grand Total	1152	220	65	194	209	183	2023			
	Propotion Percent	103.50%	102.33%	80.25%	87.78%	100.97%	98.39%		Absolute Accuracy	Within 1 facies	#Pred/#Actural F5,
	Difference	39	5	16	113	12	24	209	91.05%	94.17%	99.75%

The results of model with network size (number of hidden layers) 35 and damping parameter 0.05 for 10 key wells with PE log. The absolute accuracy for this model is 91%. For a few wells without PE curve, the results decreased but an absolute accuracy of approximately 85% was still attained.

Predicted Lithofacies Results for 10 Key Cored Wells

Model With PE Curves

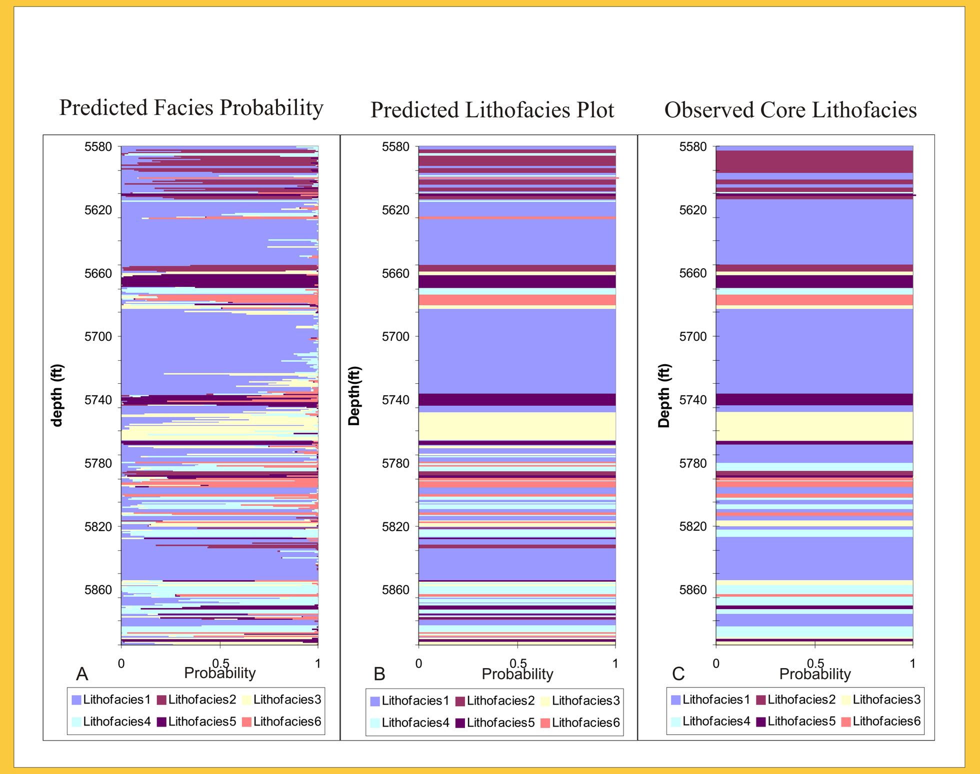

[1] Kansas Geological Survey, University of Kansas, Lawrence, KS
[2] Present Address: Chevron Energy Technology Company, San Ramon, CA
[3] Department of Geology, University of Kansas, Lawrence, KS

STRATIGRAPHY & STRUCTURE

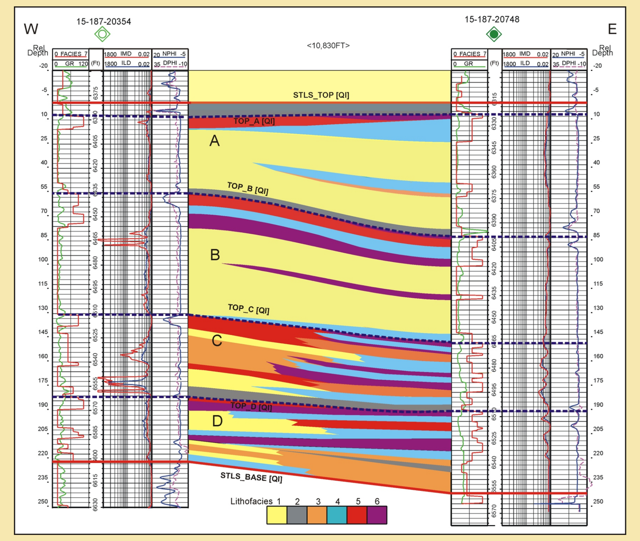

Color-filled cross section of interpolated lithofacies between well L. E. Nordling 1 and Federal Land Bank 5-21 with predicted lithofacies curves. Quartz-rich carbonate grainstone (lithofacies 1) dominates in the St. Louis A and B zones. Ooid grainstone (lithofacies 5) defines informal reservoir intervals "A" through "D". Predicted lithofacies curves were integrated with log marker and patterns to correlate St. Louis Limestone zone tops. Interpreted flooding surfaces shown as dashed lines. Facies distribution between wells based on simple 2D interpolation.

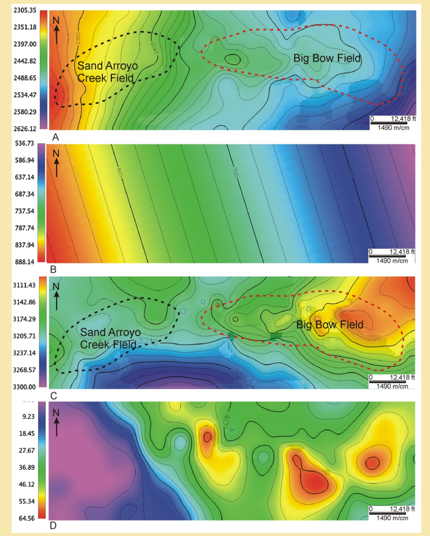

A) Structural map of St. Louis Limestone, constructed from wells surrounding Big Bow and Sand Arroyo Creek fields. Outlines of Big Bow and Sand Arroyo Creek are shown. B) Structural map of Fort Riley Limestone, showing the regional tilting effect of the Laramide Orogeny. C) Restored structural map of St. Louis Limestone constructed after removing the tilting effect of the Laramide Orogeny. Outlines of Big Bow and Sand Arroyo Creek are shown. D) Isopach map of St. Louis Limestone calculated from original structural top and base surfaces of St. Louis Limestone.

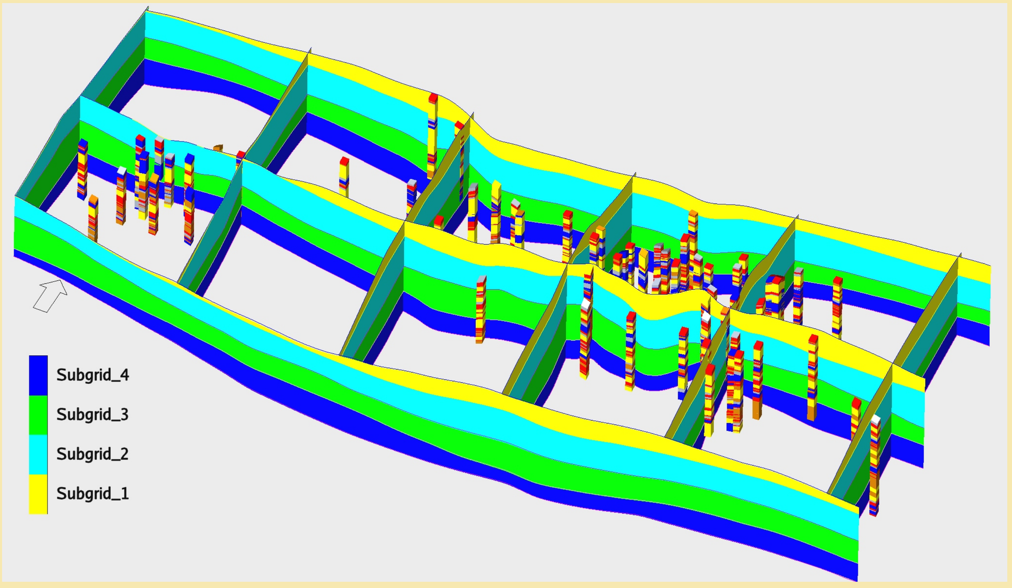

Three-dimensional fence diagram through the modeling grid at X axis (1, 26, 51, 76, 101, 126) and Y axis (1, 22, 43), showing four subgrids with the blocked wells. Facies curves are displayed on the wells. Vertical exaggeration is 40.

OBJECT-BASED SIMULATION

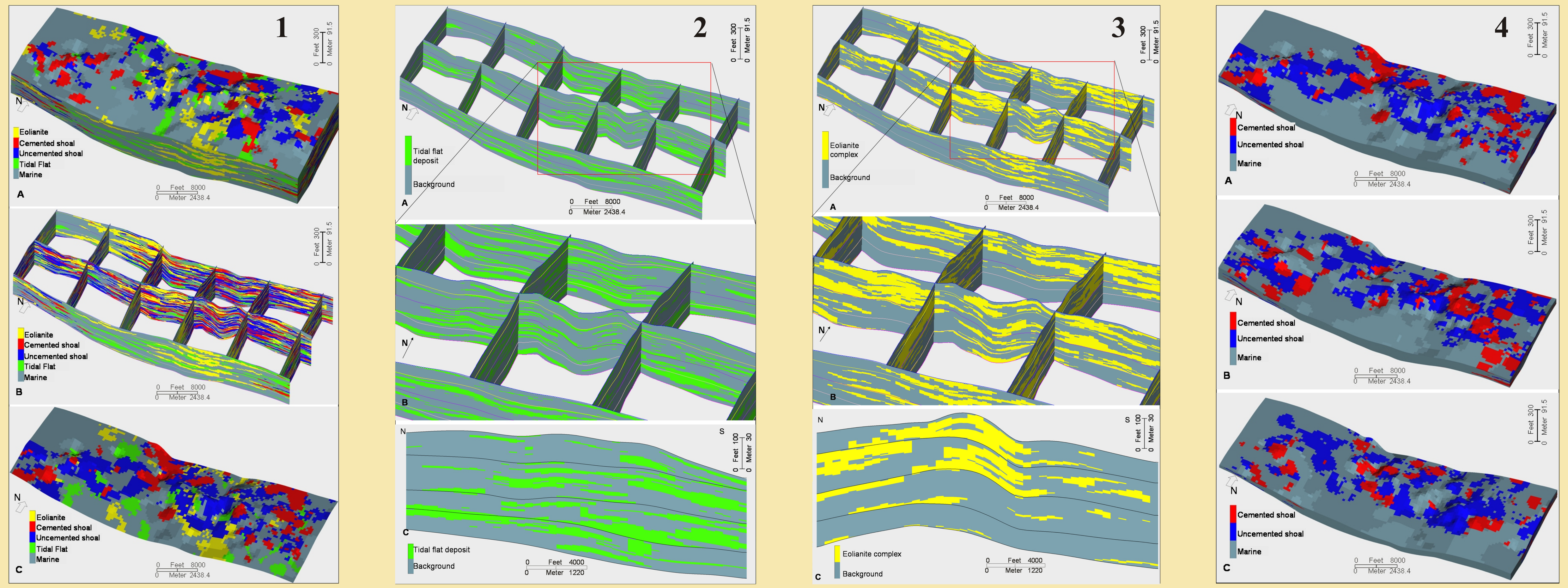

1 - A) Stochastic facies model using object-based simulation, St. Louis Limestone. B) Three-dimensional cut slices at X axis (1, 26, 51, 76, 101, 126) and Y axis (1, 22, 43); C) Top view of St. Louis B zone, layer = 38. Vertical exaggeration is 40.

2 - A) Stochastic simulation of distribution of tidal flat facies in the St. Louis Limestone; B) Zoom-in view showing detailed distribution of tidal flat facies; C) The cross section at X=122. The modeled tidal flat deposit occurs as relatively thin layers that are more laterally persistent than other two facies. The content of tidal flat deposit decreases from the bottom to the top within each zone, which may indicate of transgression and then agradation of shallow marine facies. Tidal flats preferentially accumulate in the structure lows. Three-dimensional fence diagram at X axis (1, 26, 51, 76, 101, 126) and Y axis (1, 22, 43). Vertical exaggeration is 40.

3 - A) Stochastic simulation of distribution of eolianite deposits of St. Louis Limestone; B) Zoom-in view showing the detailed distribution pattern of eolianite deposits; C) The cross section at X=63. The content of eolianite complexes increases from the zone D through zone A. Eolianite deposits show a back-stepping pattern. Three-dimensional fence diagram at X axis (1, 26, 51, 76, 101, 126) and Y axis (1, 22, 43). Vertical exaggeration is 40.

4 - A) Stochastic facies model of oolitic deposit complex and cemented oolitic deposits of zone B, St. Louis Limestone; B) Stochastic facies model of oolitic deposit complex and cemented oolitic deposits of zone C, St. Louis Limestone; C) Stochastic facies model of oolitic deposit complex and cemented oolitic deposits of zone D, St. Louis Limestone. Oolitic deposits accumulate on the local highs surrounding the embayment. Vertical exaggeration is 40.

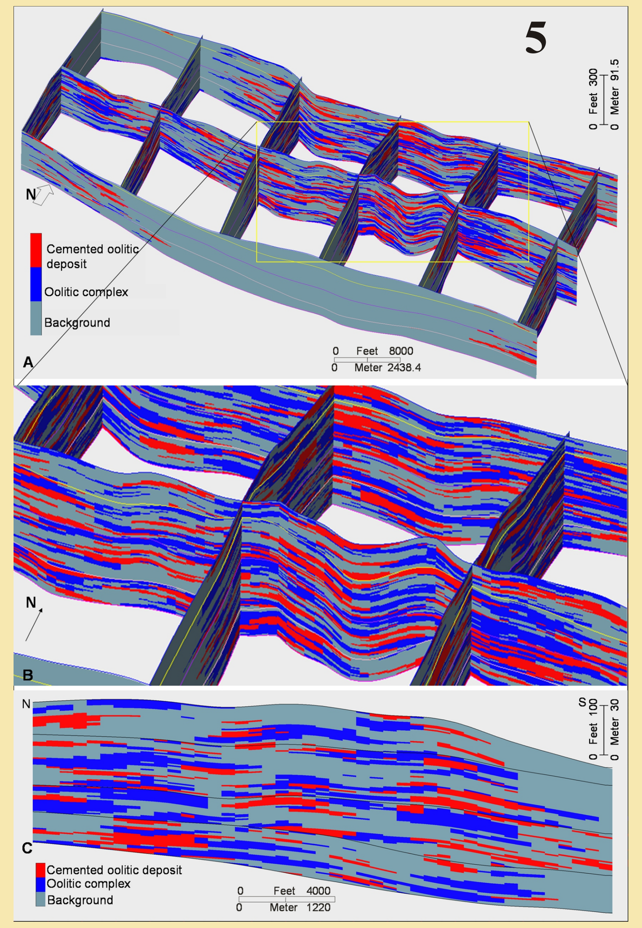

5 - A) Stochastic simulation of distribution of ooid deposit complexes (lithofacies 5 and 6) and cemented oolitic deposits (lithofacies 6) of St. Louis Limestone. Oolitic complexes show an agradational pattern accumulating along the edge of the deeper embayment in south; B) Zoom-in views showing detailed distribution pattern of cemented oolitic deposits (red) within the oolitic complexes (blue); C) The cross section at X=122, showing that cementation of oolitic deposits tends to occur at the edges of shoal complexes. Shoal complexes are largely absent on the high in the northwest corner of the study area and in the deeper parts of the study area to the south. Oolitic complexes display a progradational pattern within each zone. Three-dimensional fence diagram at X axis (1, 26, 51, 76, 101, 126) and Y axis (1, 22, 43). Vertical exaggeration is 40.